Green's function solution to the tissue bioheat equation

Reeta Vyas
Department of Physics, University of Arkansas, Fayetteville, Arkansas 72701

M. L. Rustgi
Department of Physics, State University of New York at Buffalo, Buffalo, New York 14260

(Received 18 October 1991; accepted for publication 13 May 1992)

A Green's function solution to the tissue bioheat equation including blood flow in cylindrical geometry is obtained. Numerical results for temperature variation in the bovine muscle are reported when the tissue is exposed to neodymium–yttrium–aluminum garnett (Nd:YAG) lasers with Gaussian profile and a comparison with recent measurements is made. A strong dependence of the tissue temperature on the beam radius and pulse time is found.

I. INTRODUCTION

The influence of lasers in biological and medical research is becoming increasingly important.[1–8] The neodymium–yttrium–aluminum garnett (Nd:YAG) laser, which is capable of being operated as either pulsed or continuous wave (cw), with pulse widths varying, with mode of operation, from nanoseconds to picoseconds and power to the order of 10^{10} W has eclipsed the use of ruby laser. The Nd:YAG laser finds most of its application in the utilization of its 1064-nm light. The laser tissue interaction is mainly determined by two parameters, the interaction time of the radiation with the tissue and the effective energy density which brings about an effect whereby the tissue-specific absorption must be taken into consideration. At low energy density with a long exposure the absorption of light primarily leads to photochemical processes. With decreasing interaction time and higher energy densities is the domain of the photothermal-induced effects. In this paper, a Green's function solution to the tissue bioheat equation is obtained to describe the temperature distribution due to a laser beam with Gaussian profile. The effect of thermal conduction on the temperature decay curve within the framework of the bioheat equation has been investigated by Sandhu,[1] who pointed out that in limited cases, the decay curve may be used to measure blood flow. Though the solution of the bioheat equation on excluding blood flow has been obtained by a number of authors,[2–7] the Green's function approach used here is quite general and includes the blood flow in the solution of the bioheat equation.

In Sec. II simple analytical expressions for Green's function and temperature distribution using a model with cylindrical symmetry are derived. The heat source is assumed to be a pulsed laser beam with a Gaussian profile. The method is sufficiently general to enable calculation of temperature distribution for other sources with cylindrical symmetry such as cw laser using this Green's function. In Sec. III results are compared with available experimental data.[8]

II. GREEN'S FUNCTION AND TEMPERATURE DISTRIBUTION

In this section, an expression for the temperature distribution $T(r,z,t)$ in a tissue that is exposed to the laser beam is derived. The derivation is based on a cylindrically symmetric model in which the laser beam is traveling in the z direction. The temperature distribution for this system is described by a differential equation which is essentially an equation of energy conservation. The Green's function approach is followed to solve the differential equation for the temperature distribution. Since the Green's function obtained for the differential equation is independent of the source term, the same Green's function can be used to calculate temperature distribution for various sources with different spatial and temporal profiles. Even though this problem is solved for a cylindrically symmetric system, this approach can be extended to calculate the temperature distributions for systems that do not possess cylindrical symmetry.

The bioheat equation was first proposed by Pennes[9] and the inherent assumptions in this equation are outlined in Hodson *et al.*[10] The differential equation describing the temperature distribution can be written as[9,10]

$$\frac{\partial T(r,z,t)}{\partial t}=D\nabla^2 T(r,z,t)-bT(r,z,t)+\frac{1}{\rho C}S(r,z,t), \quad (1)$$

where the first and the second terms on the right-hand side of Eq. (1) are due to the thermal diffusion and blood flow, the temperature above the baseline temperature of the tissue is $T(r,z,t)$, $S(r,z,t)$ is the power deposited per unit volume due to the absorption of the laser energy, the thermal diffusivity D is equal to $\kappa/\rho C$, where κ, ρ, and C are thermal conductivity, density, and specific heat of the tissue, respectively. The parameter b is given by $\omega\rho_b C_b/C$. Here ω is volumetric blood flow, C_b is the specific heat of the blood, and ρ_b is density of the blood. The boundary conditions imposed on the temperature and its derivatives are that they vanish as r and z go to infinity. These boundary conditions require that the source energy must vanish at infinity. It is also assumed that at time $t=0$, the temperature is zero. The solution of Eq. (1) can be expressed in terms of Green's function $G(r,z,t;r',z',t')$ and the source term $S(r,z,t)$ as[11]

$$T(r,z,t)=\int_0^\infty\int_{-\infty}^{\infty}\int_{-\infty}^{\infty}S(r',z',t')G(r,z,t;r',z',t')\times r'dr'dz'\,dt'. \quad (2)$$

 0094-2405/92/51319-06$01.20

Here the Green's function $G \equiv G(r,z,t;r',z',t')$ is solution of the differential equation,

$$\frac{\partial G}{\partial t} - D\left(\frac{\partial^2 G}{\partial r^2} + \frac{1}{r}\frac{\partial G}{\partial r} + \frac{\partial^2 G}{\partial z^2}\right) + bG = \frac{1}{\rho C}\delta(r-r')\delta(z-z')\delta(t-t'), \tag{3}$$

subjected to the same boundary conditions as imposed on the temperature $T(r,z,t)$. In order to solve Eq. (3) we first take the Hankel Transform[11] of Eq. (3) with respect to the r coordinate:

$$\frac{\partial G_h}{\partial t} - D\left(\frac{\partial^2 G_h}{\partial z^2} - k^2 G_h\right) + bG_h = \frac{r'}{\rho C} J_0(kr')\delta(z-z')\delta(t-t'), \tag{4}$$

where

$$G_h \equiv G_h(k,z,t;r',z',t') = \int_0^\infty G(r,z,t;r',z',t') J_0(kr) r\, dr. \tag{5}$$

Next we perform the Fourier Transform[11] of Eq. (4) with respect to the z coordinate which yields

$$\frac{\partial G_{hf}}{\partial t} + D(k_z^2 + k^2)G_{hf} + bG_{hf} = \frac{r'}{\sqrt{2\pi}\rho C} J_0(kr') e^{ik_z z'}\delta(t-t'), \tag{6}$$

where

$$G_{hf} \equiv G_{hf}(k,z,t;r',z',t') = \frac{1}{\sqrt{2\pi}} \int_{-\infty}^{\infty} G_h(r,z,t;r',z',t') e^{ik_z z}\, dz. \tag{7}$$

The Laplace Transform[11] of Eq. (6) results in an algebraic equation for G_{hfl}, the Laplace Transform of G_{hf}. On simplifying that algebraic equation, we obtain

$$G_{hfl} = \frac{r' J_0(kr') e^{ik_z z'} e^{-st'}}{\sqrt{2\pi}\rho C[s + b + D(k^2 + k_z^2)]}, \tag{8}$$

where G_{hfl} is given by

$$G_{hfl} \equiv G_{hfl}(k,z,t;r',z',t') = \int_0^\infty G_{hf}(r,z,t;r',z',t') e^{-st}\, dt. \tag{9}$$

The function G_{hf} can be obtained by taking the inverse Laplace transform of Eq. (8) and can be written as

$$G_{hf} = \frac{r' H_{t'}(t)}{\sqrt{2\pi}\rho C} J_0(kr') e^{ik_z z'} \exp\{-[b + D(k^2 + k_z^2)] \times (t-t')\}. \tag{10}$$

Here, $H_{t'}(t)$ is unit step function defined as

$$H_{t'}(t) = 1, \quad t > t', \qquad = 0, \quad t < t'. \tag{11}$$

On performing an inverse Fourier transform of Eq. (10), we obtain the function G_h in the form

$$G_h = \frac{r' H_{t'}(t)}{2\rho C\sqrt{\pi D(t-t')}} J_0(kr') \exp\left(-\frac{(z-z')^2}{4D(t-t')}\right) \times \exp[-(b + Dk^2)(t-t')]. \tag{12}$$

Finally the Green's function G is obtained by taking the inverse Hankel transform of Eq. (12):

$$G = \frac{r' H_{t'}(t)}{\sqrt{2\pi}\rho C[2D(t-t')]^{3/2}} \exp[-b(t-t')] \times \exp\left(-\frac{(z-z')^2}{4D(t-t')}\right) \times \exp\left(-\frac{(r^2 + r'^2)}{4D(t-t')}\right) I_0\left(\frac{rr'}{2D(t-t')}\right). \tag{13}$$

Here, I_0 is the modified Bessel function of order zero.[11,12] On substituting the Green's function and the source function in Eq. (2) the temperature distribution in the medium is obtained.

We now consider a pulsed laser source which is placed at the origin with the laser beam propagating in the z direction. The intensity of the laser beam has Gaussian spatial profile and is decaying exponentially in the z direction. A Gaussian profile is a good approximation for many laser sources available in the laboratory and for this profile the temperature distribution can be expressed analytically in a simple compact form. This simple model gives good physical insight into the problem. The source term for a Gaussian profile can be written as

$$S(r,z,t) = \alpha I(r,z,t), \qquad = \frac{2\alpha E_0}{\pi a^2 t_0} e^{-2r^2/a^2} e^{-\alpha z}, \quad z > 0, \quad \text{and} \quad t_0 > t > 0, \qquad = 0, \quad \text{otherwise.} \tag{14}$$

Here, a is the $1/e^2$ radius of the laser beam with Gaussian spatial profile, E_0 is the total energy in one pulse, and α is the absorption coefficient of the medium. The temporal profile is assumed to be rectangular with pulse duration t_0. On substituting the Green's function given by Eq. (13) and the source term given by Eq. (14) in Eq. (2) and on performing integrations over z' and r' we get[12]

$$T(r,z,t) = K\int_0^{\tau_0} dt' \frac{\exp[-b(t-t')]}{[a^2 + 8D(t-t')]} \times \exp\left(-\frac{2r^2}{a^2 + 8D(t-t')}\right) \times \exp[-\alpha z + \alpha^2 D(t-t')] \times \operatorname{erfc}\left(\frac{2D\alpha(t-t') - z}{\sqrt{4D(t-t')}}\right), \tag{15}$$

with

$$K = \alpha E_0/\pi\, t_0 \rho C. \tag{16}$$

Here, erfc(x) is the complementary error function,[11] τ_0 is the minimum of t or t_0. It is not possible to integrate analytically the right hand side of Eq. (15) over t'. We perform this integration numerically by using the Gaussian quadrature method.

For short pulses, one can make impulse approximation that is equivalent to replacing the integral by the product of integrant at zero time and time interval, i.e.,

$$\lim_{t_0 \to 0} \int_0^{t_0} f(t')dt' = f(0)t_0 .$$

In this approximation, the temperature distribution can be written as

$$T(r,z,t) = Kt_0 \frac{\exp(-bt)}{(a^2+8Dt)} \exp\left(-\frac{2r^2}{a^2+8Dt}\right) \times \exp(-\alpha z+\alpha^2 Dt)\,\mathrm{erfc}\left(\frac{2D\alpha t - z}{\sqrt{4Dt}}\right). \quad (17)$$

The curves for the approximate solution almost coincide with the curves for the exact solution for short pulses of microsecond duration. For longer pulses of few hundred microsecond duration disagreement between the exact and the approximate solutions begins to show up.

One can also integrate Eq. (15) over the radial variable r and obtain the average temperature $\langle T \rangle$, defined as[8]

$$\langle T \rangle \equiv \langle T(r,z,t) \rangle = \int_0^{\infty} T(r,z,t) r\, dr. \quad (18)$$

On substituting the expression for temperature given by Eq. (15) in Eq. (18) and performing integration over r one obtains

$$\langle T \rangle = \frac{K}{4} \int_0^{\tau_0} dt' \exp[-b(t-t')] \times \exp[-\alpha z+\alpha^2 D(t-t')]\,\mathrm{erfc}\left(\frac{2D\alpha(t-t')-z}{\sqrt{4D(t-t')}}\right). \quad (19)$$

From Eq. (19) one finds that the average temperature is independent of beam radius a and has same z dependence as for the temperature distribution. Since the average temperature is obtained by integrating temperature distribution over r coordinate, the temperature distribution contains more information than the average temperature.

III. RESULTS AND DISCUSSIONS

In this section, results for temperature and average temperature distributions are obtained for bovine muscle and liver tissues by using Eqs. (15) and (19), respectively. Gaussian quadrature method is used to integrate over t' variable numerically. The parameters which affect the temperature distribution are the thermal diffusivity D, beam radius a, absorption coefficient α, and constant K (depends upon laser power, α, density and specific heat of the medium). Typical values of these parameters for the plots are taken from Refs. 1 and 8.

In Fig. 1 temperature T is plotted as a function of radial distance r for bovine muscle (lower curve) and bovine liver (upper curve) tissues. The experimental points are taken from Ref. 8. The solid curves are theoretical curves drawn by using Eq. (15). Numerical values of various parameters[1,8] chosen for computation are, laser power $E_0/t_0 = 70$ W, pulse duration $t_0 = 0.3$ s, time $t = 5$ s, distance $z = 1$ mm, thermal diffusivity $D = 0.12$ (mm^2 s^{-1}), $b = 0.0013$ (s^{-1}), constants $K = 3.5 \times 10^{-4}$ (m^2 °C/s) (muscle) and 4.64×10^{-4} (m^2 °C/s) (liver), absorption coefficients $\alpha = 0.06$ (mm)$^{-1}$ (muscle) and 0.08 (mm)$^{-1}$ (liver), and beam radius $a = 4.5$ mm (muscle) and 4.2 mm (liver). In the short pulse approximation beam radius "a" is related to the corresponding parameter "b" of Ref. 8 as $[a^2+8Dt]/2$ and values "a" obtained for Fig. 1 are in good agreement with the corresponding parameter of Grossweiner *et al.*

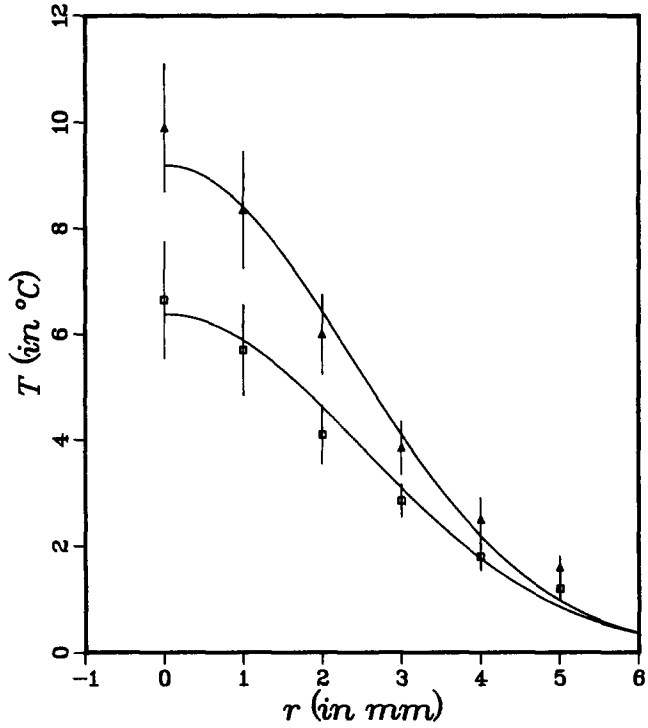

FIG. 1. Temperature distribution for bovine muscle and liver tissues as a function of r for $t = 5$ s and $z = 1$ mm. Experimental points are from Grossweiner *et al.*[8] Theoretical curves are plotted from Eq. (15) for the parameters listed in Sec. III.

In Figs. 2 and 3 temperature T is plotted as a function of time t for radial distances $r = 0$ and 3 mm, respectively. Various curves are for different z values: 1 mm (solid), 3 mm (dot), 5 mm (dash), and 1 cm (dash-dot). For these curves the beam radius a is chosen to be 2.1 mm and all the other parameters are chosen to be same as those for bovine tissue (Fig. 1). On comparing Figs. 2 and 3 it is noticed that temperature decreases very rapidly outside the beam radius. This is so because the thermal diffusivity is very small and therefore very little heat diffuses outside the beam radius. Also since the parameter b is very small, its effect on the temperature distribution is negligible. Maximum temperature for these parameters is achieved at time $t = t_0 = 0.3$ s, $r = 0$, and $z \approx 1$ mm. Comparing Figs. 1 and 2

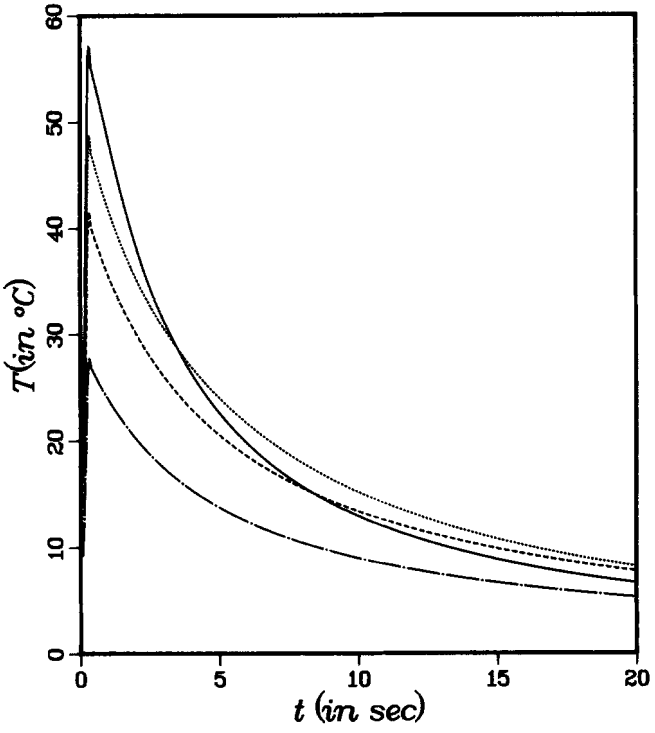

FIG. 2. Temperature distribution for bovine liver tissue as function of time t for $r=0$, $t_0=0.3$ s, $a=2.1$ mm, and z values 1 mm (solid), 3 mm (dot), 5 mm (dash), and 10 mm (dash-dot). Other parameters are same as those for Fig. 1.

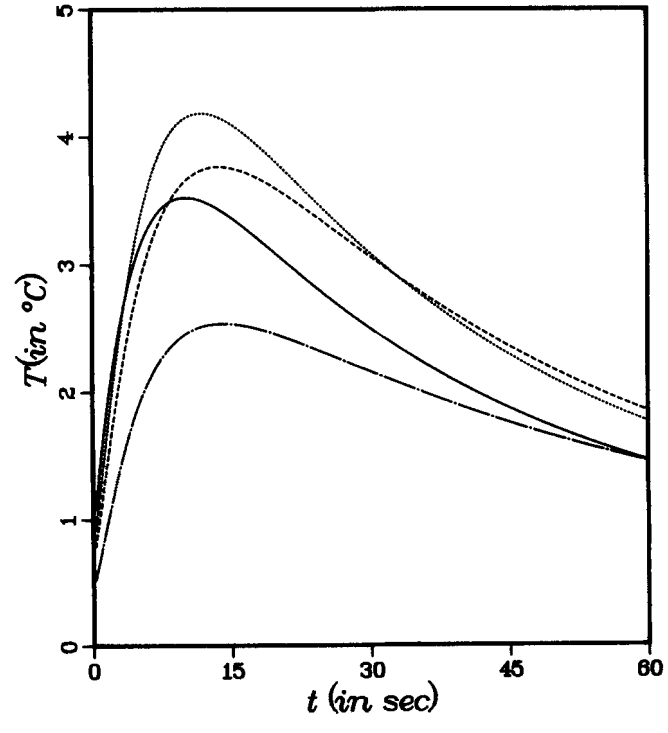

FIG. 3. Temperature distribution for bovine liver tissue as function of time t for $r=3$ mm, $t_0=0.3$ s, $a=2.1$ mm, and z values 1 mm (solid), 3 mm (dot), 5 mm (dash), and 10 mm (dash-dot). Other parameters are same as those for Fig. 1.

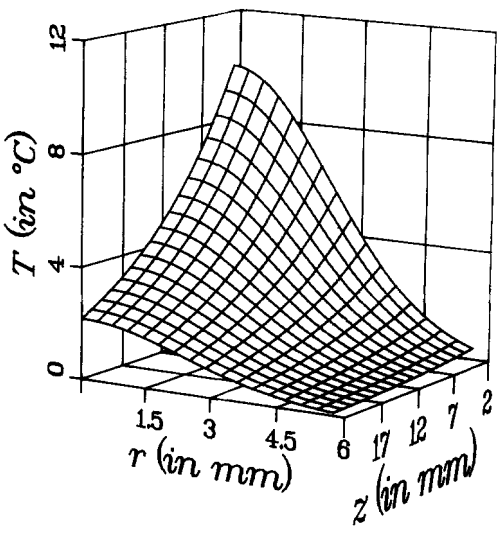

FIG. 4. Temperature distribution for bovine liver tissue as function of r and z at time $t=5$ s. Other parameters are same as those for Fig. 1.

we notice that maximum temperature achieved is very sensitive to the value of beam radius a. With decrease in beam radius maximum temperature increases very rapidly. It is approximately inversely proportional to the square of the beam radius a and directly proportional to the pulse duration t_0.

Fig. 4 shows a three-dimensional plot of temperature as a function of r and z at time $t=5$ s. Parameters used for the plot are same as those used for bovine tissue in Fig. 1. Along the r axis temperature has approximately Gaussian distribution whose width increases with time t. For short pulses, this width is given by $(a^2+8Dt)/2$. Along the z-axis temperature initially increases with increase in z because of the erfc term in Eq. (15), but as z increases further the exponential term in Eq. (15) dominates and temperature decreases exponentially. The initial increase in temperature with increase in z is due to the heat lost by diffusion to region where no heat source is present. In the absence of diffusion ($\lim_{D\to 0}$) temperature decays exponentially with increase in z.

In Fig. 5, values of $\langle T\rangle$ are plotted as function of distance z for muscle and liver tissues and are compared with the experimental results of Grossweiner *et al.*,[8] who obtained these results by numerically integrating the experimental temperature distribution over the radial variable r. Best theoretical fits to these experimental points are obtained with $K=3.5\times10^{-4}$ (m^2 °C/s) (muscle) and 5.33×10^{-4} (m^2 °C/s) (liver), $\alpha=0.13$ $(mm)^{-1}$ (muscle) and 0.2 $(mm)^{-1}$ (liver), $t_0=0.3$ s, $D=0.22$ ($mm^2\,s^{-1}$), and $b=0.0013$ (s^{-1}). The values of α for the best theoretical curves are found to be slightly higher than the straight line fit of Ref. 8 for exponential decay because of the erfc term. In our work, we do not make the assumption that average temperature decays exponentially as a function of z, but the z dependence of the temperature emerges naturally on solving the differential equation for temperature. Just like the temperature curve of Fig. 4, the increase in

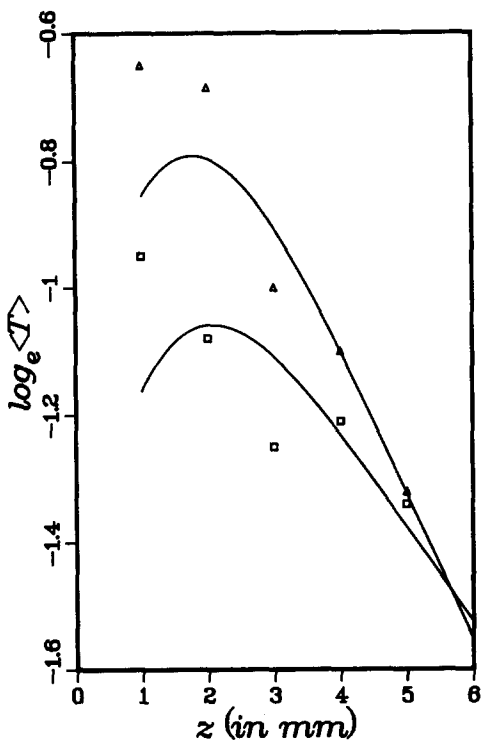

FIG. 5. Log_e of average temperature distribution for bovine muscle and liver tissues as a function of z for time $t=5$ s. The average temperature distribution is in units of cm^2 °C. Other parameters are listed in Sec. III. Experimental points are from Grossweiner *et al.*[8] for muscle (square) and liver (triangle) tissues.

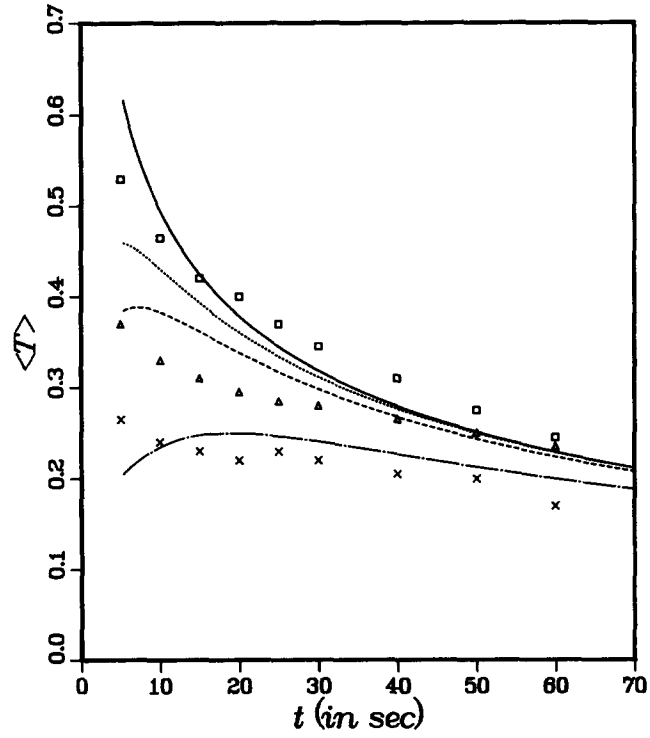

FIG. 6. Average temperature distribution in units of cm^2 °C for bovine liver tissue as a function of time t for various z values: 1 mm (solid), 3 mm (dot), 4 mm (dash), and 5 mm (dash-dot). Other parameters are listed in Sec. III. Experimental points are from Grossweiner *et al.*[8] for $z=1$ mm (square), 3 mm (triangle), and 5 mm (cross).

calculated $\langle T \rangle$ with increase in z is due to the erfc term in Eq. (18), but for large z values the exponential term dominates resulting in an exponential decay of the average temperature. This temperature buildup with z is also enhanced by the optical properties which have been used since the attenuation coefficient is so small.

The average temperature $\langle T \rangle$ for different depths in bovine liver is plotted as function of time t in Fig. 6. The experimental points are the average of three independent measurements at $z=1$, 3, and 5 mm and are taken from Ref. 8. The theoretical curves are obtained for $K=1.04\times10^{-3}$ (m^2 °C/s), $\alpha=0.45$ $(\text{mm})^{-1}$, $D=0.22$ ($\text{mm}^2\,\text{s}^{-1}$), and $b=0.0013$ (s^{-1}). The various values of z are chosen to be 1 mm (line), 3 mm (dot), 4 mm (dash), and 5 mm (dash-dot). It is found that a reasonable fit to these points can be obtained for α ranging from 0.41 $(\text{mm})^{-1}$ to 0.55 $(\text{mm})^{-1}$ by slightly adjusting the constant K. On the other hand these curves are found to be very sensitive to the values of z for one can notice that the theoretical curve for $z=4$ mm provides a better fit to the experimental data for $z=3$ mm than the calculated curve for $z=3$ mm. In Ref. 8, the time dependence of $\langle T \rangle$ is derived by imposing the surface convection boundary condition at $z=0$, which introduces a new parameter in the expression for the average temperature distribution, and leads to more complex expression for the temperature distribution. The boundary condition that the temperature vanishes at infinity, which is imposed in this work results in a simple analytical expression for the temperature distribution. From Eq. (18), it is seen that in the long time limit the log of average radial temperature is proportional to $1/\sqrt{t}$, in agreement with Ref. 8.

In conclusion, we have obtained simple analytical expressions for the temperature and average temperature distribution by using the Green's function approach. The Green's function derived here can be used to obtain temperature distribution for other temporal and cylindrically symmetric spatial profile. Theoretical results are in good agreement with the experimental results of Grossweiner *et al.* [8]

ACKNOWLEDGMENTS

The work of one of the authors (RV) was supported in part by grants from Arkansas Science and Technology Authority (ASTA). The other author (MLR) is grateful to Dr. D. J. Nagel of the Naval Research Laboratory for his interest in this work.

[1] T. S. Sandhu, "Measurement of blood flow using temperature decay: Effect of thermal conduction," Int. J. Radiation Oncology Biol. Phys. **12**, 373 (1986).
[2] M. J. C. Van Gemert and A. J. Welch, "Time constants in thermal laser medicine," Lasers Surg. Med. **9**, 405 (1989).
[3] M. J. C. Van Gemert, W. J. deKleijn, and J. P. Hulsbergen Henning, "Temperature behavior of a model portwine stain during argon laser coagulation," Phys. Med. Biol. **27**, 1089 (1982).

[4]R. Birngruber, "Thermal modeling in biological tissues," in *Lasers in Biology and Medicine*, edited by F. Hillenkamp, R. Pratesi, and C. A. Sacchi (Plenum, New York, 1980) pp. 77–97.
[5]L. A. Priebe and A. J. Welch, "A dimensionless model for the calculation of temperature increase in biological tissues exposed to nonionizing radiation," IEEE Trans. Biomed. Eng. **26**, 244 (1979).
[6]E. H. Wissler, "An analysis of choroid-retinal thermal response to intense light exposure," IEEE Trans. Biomed. Eng. **23**, 207 (1976).
[7]A. N. Takata, "Development of criterion for skin burns," Aerospace Med. **45**, 637 (1974).
[8]L. I. Grossweiner, A. M. Al-Karmi, P. W. Johnson, and K. R. Brader, "Modeling of tissue heating with a pulsed Nd:YAG laser," Lasers Surg. Med. **10**, 295 [Wiley-Liss, New York (1990)]; L. I. Grossweiner, James L. Karagiannes, P. W. Johnson, and Z. Zhang, App. Opt. **29**, 379 (1990).
[9]H. H. Pennes, "Analysis of tissue and arterial temperatures in the resting human forearm," J. Appl. Physiol. **1**, 93 (1948).
[10]D. A. Hodson, G. Eason, and J. C. Barbenel, "Modeling transient heat transfer through the skin and superficial tissues: surface insulation," Trans. ASME J. Biomech. Eng. **108**, 183 (1979).
[11]G. Arfken, *Mathematical Methods for Physicists* (Academic, New York, 1985).
[12]I. S. Gradshteyn and I. M. Ryzhik, *Tables of Integrals, Series, and Products* (Academic, New York, 1965).